ISBN: 978-3-95450-184-7 doi:10.18429/JACoW-IPAC2018-MOPML066

ULTRAFAST MEGA-ELECTRON-VOLT GAS-PHASE ELECTRON DIFFRACTION AT SLAC NATIONAL ACCELERATOR LABORATORY*

Xiaozhe Shen, Jie Yang, Renkai Li, Stephen Weatherspy and Xijie Wang
SLAC National Accelerator Laboratory, Menlo Park, CA 94025, USA

Abstract

Ultrashort mega-electron-volt (MeV) electron beams from radio-frequency (rf) photoinjectors have recently attracted strong interests for application in ultrafast gas-phase electron diffraction (UGED). Such high-brightness electron beams are capable of providing 100-fs level temporal resolution and sub-Angstrom level spatial resolution to capture the ultrafast structural dynamics from photoexcited gas molecules. To experimentally demonstrate such an ultrafast electron scattering instrument, a high performance UGED system has been commissioned at SLAC National Accelerator Laboratory. The UGED instrument produces 3.7 MeV electron beams with 2 fC beam charge at 180-Hz repetition rate. The temporal resolution is characterized to be 150 fs full-width-at-half-maximum (FWHM), while the spatial resolution is measured to be 0.76 Å FWHM. The UGED instrument also demonstrates outstanding performance in vacuum, rf, and electron beam pointing stability. Details of the performance of the SLAC MeV UGED system are reported.

INTRODUCTION

The advent of high-brightness electron source has greatly promoted the development of cutting-edge scientific instruments, such as x-ray free electron lasers [1,2] and inverse Compton scattering devices [3]. In particular, mega-electron-volt (MeV) electron beams from high-brightness radio-frequency (rf) photoinjectors have shown great potentials [4,5] for application in ultrafast electron diffraction (UED) [6] and microscopy (UEM) [7]. The space-charge forces for such electrons at relativistic energies are greatly suppressed, which offers great opportunities to achieve a bunch length at 100-fs level to reach the ultrafast atomic time scale. The de Broglie wavelength of MeV electrons reaches sub-picometer level, which provides direct access to atomic length scale. The high elastic scattering cross section makes MeV electron an efficient probe for structural changes in matter. Over the last decades, numerous research and development efforts have been devoted to application of MeV electrons for UED/UEM [8-16].

Gas phase diffraction experiments focus on probing atomic motions of isolated molecules underwent photoexcitation, such as molecular rotation, vibration, ring-opening, and bond-breaking. The underlying dynamics occurs over a typical time scale of $\leq$ 100 fs, and a typical length scale of a few Å [17]. Thanks to the high scattering cross section and high spatial resolution, electrons at non-relativistic energies have been successfully applied for gas phase electron diffraction and bloomed remarkable scientific results, but the temporal resolution remains in picosecond level [18-20]. Implementing electron beams at relativistic electron energies is an effective approach to produce ultrashort high-brightness electron beams to break the temporal resolution barrier and realize ultrafast gas phase electron diffraction (UGED). Based on the MeV UED beamline at SLAC National Accelerator Laboratory [15, 16], an MeV UGED system was experimentally commissioned and a temporal resolution of 250 fs full width at half maximum (FWHM) [21] was demonstrated.

The performance of the SLAC UGED system has been recently optimized to achieve a 150 fs FWHM temporal resolution as well as ultrahigh machine stabilities. In this paper, the experimental set up of the upgraded SLAC MeV UGED system is reported. Experimental characterizations of instrumental resolutions and machine stabilities are presented.

EXPERIMENTAL SET UP OF THE SLAC MEV UGED SYSTEM

Figure 1 shows a schematic of the SLAC MeV UGED beamline. The electron source is a S-band 1.6-cell photocathode rf gun, which is identical to that for the Linac Coherent Light Source injector [1]. The gun solenoid is directly mounted to the exit of the rf gun to ensure good alignment. The gun ion pump monitors the ultrahigh vacuum in the rf gun. The diagnostic cross contains a profile monitor for beam diagnostics, a movable Faraday cup for beam charge measurement, and a motorized collimator with apertures of 100, 200, and 500 μm diameter. The differential pumping section consists of an ion pump and beam pipes much smaller than those on both upstream and downstream sides. It creates a vacuum isolation between upstream and downstream beamlines to protect the ultrahigh vacuum in the rf gun. The micro focusing solenoid adds additional freedom for beam focusing control. The ancillary turbo pump serves as a second differential pumping stage before the gas chamber. Gas pulses are injected from the gas nozzle and pumped out of the gas chamber by the chamber turbo pump. The electron detector system is a phosphor-screen based charge coupled device.

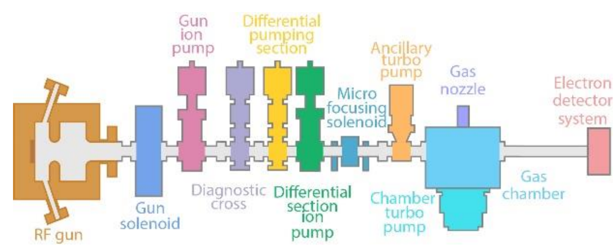

Figure 1: Schematic of the MeV UGED beamline at SLAC National Accelerator Laboratory.

ISBN: 978-3-95450-184-7 doi:10.18429/JACoW-IPAC2018-MOPML066

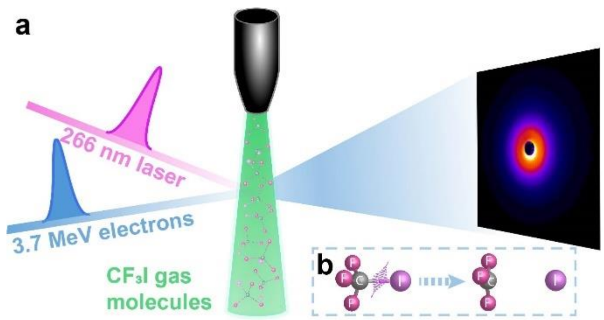

Figure 2: Schematic of a typical set up for laser-pump-electron-probe gas-phase diffraction experiment (a) to study the ultrafast structural dynamics of CF_3I photodissociation (b).

Figure 2a shows a schematic of a typical set up for laser-pump-electron-probe gas phase diffraction experiment, with CF_3I photodissociation as an exemplar dynamical process. The CF_3I molecules ejected from the gas nozzle are excited by the 266 nm laser. As shown in Fig. 2b, the C-I bond is broken upon the laser excitation, and the I fragment quickly departs from the CF_3 fragment. The 3.7 MeV electron beams capture the snapshot of this dynamical process and imprint the information onto the diffraction pattern formed on the electron detector. By varying the arrival time delay between the laser and the electron pulses, the whole dynamical process can be time-resolved from the diffraction pattern series.

The SLAC MeV UGED system is equipped with a Ti:Sapphire laser system which produces 50 fs laser pulses at 800 nm wavelength with 3.2 mJ pulse energy. 0.6 mJ of the 800 nm laser pulse is converted to 266 nm to drive the rf gun photocathode to generate photoelectrons. The other 2.6 mJ pulse is reserved for generation of pump laser. A low level rf-laser timing system and a high stability rf power source control the root-mean-square (rms) pump-probe timing jitter to be <50 fs [15]. Typical machine parameters for the SLAC MeV UGED system is summarized in Table 1.

Table 1: Typical Parameters of the SLAC MeV UGED

Parameter	Value
Repetition rate	180 Hz
Launching/delivered beam charge	10/2 fC
Collimator diameter	200 µm
Kinetic beam energy	3.7 MeV
Bunch length	<150 fs
Spatial resolution	0.76 Å
Reciprocal-space resolution	0.22 $Å^{-1}$
FWHM Beam/pump laser/gas size at interaction point	200/200/300 µm
Normalized emittance	4.5 nm-rad
Gun/gas chamber vacuum	4×10^{-10} / 5×10^{-5} torr
RMS rf amplitude stability	0.025%
RMS rf phase stability	0.032 deg
Electron beam pointing jitter	< 10 µm

INSTRUMENTAL RESOLUTIONS CHARACTERIZATION

Reciprocal-space resolution determines the finest feature that can be resolved in a diffraction pattern. With a high quality single crystal, such as Au, reciprocal-space resolution is dominated by the electron beam size on the detector. Figure 3a shows a typical diffraction pattern from Au single crystal. The FWHM width of the intensity distribution of the (200) order peaks are fitted to a Gaussian profile to be 0.22 $Å^{-1}$, which gives an estimation of the reciprocal space resolution.

Spatial resolution demv termines the finest resolvable features in real space, which is corresponding to the resolvable features with the biggest momentum transfer in the reciprocal space. The inset of Fig. 3b shows a diffraction pattern from CF_3I gas molecules. Diffraction features are resolved up to 8.3 $Å^{-1}$, which gives a spatial resolution of 0.76 Å.

The instrumental temporal resolution can be estimated from the time-resolved ultrafast photodissociation process in CF_3I gas molecules. The structural change during the photodissociation process causes corresponding changes in the diffraction pattern. Fig. 3b shows the evolution of the total intensities within the highlighted area of the CF_3I diffraction pattern in the inset. Fitting the data to an error function profile gives an estimation of 149 fs as the upper limit for the temporal resolution.

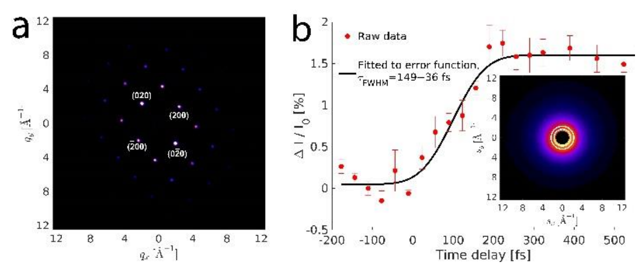

Figure 3: Reciprocal-space and temporal resolution estimation. Panel a) shows a typical diffraction pattern from Au single crystal. The FWHM width of the highlighted (200) order peaks gives an estimation of 0.22 $Å^{-1}$ for the reciprocal-space resolution. Panel b) shows the relative intensity change within the highlighted area of the CF_3I diffraction pattern (inset) during a photodissociation process. The fitting result shows an estimated FHWM temporal resolution of 149 fs.

MACHINE STABILITY PERFORMANCE CHARACTERIZATION

Vacuum Stability

In a gas phase diffraction experiment, higher gas pressure is preferred to maximize the diffraction signal induced by structural changes. However, operation of the rf photocathode gun requires an ultrahigh vacuum environment. Vacuum isolation between the rf gun and the gas chamber with high reliability is extremely important for a

ISBN: 978-3-95450-184-7 doi:10.18429/JACoW-IPAC2018-MOPML066

UGED instrument. With the carefully designed differential pumping stages in the SLAC MeV UGED system, a 5-order-of-magnitude vacuum isolation is achieved between the gas chamber and the rf gun. Figure 4 shows typical records of vacuum level in the gas chamber and the rf gun during a gas-phase experiment. The frequent changes of the gas chamber vacuum in the first 3 hours of the run is due to testing of the system. Later, the chamber vacuum had been stably sitting at around 2.5×10^{-5} torr. The rf gun vacuum had been stably fixed at 4×10^{-10} torr over the whole time scope of the experiment.

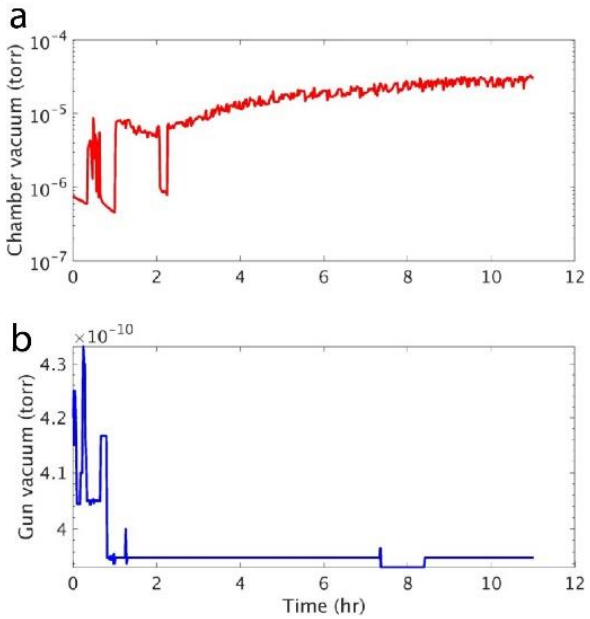

Figure 4: Typical records of vacuum level in the gas chamber (a) and rf gun (b) during a gas-phase experiment.

RF Stability

High stability in rf amplitude and phase is crucial for an rf photocathode gun to deliver high quality electron beams, with minimized time-of-arrival-jitter between the electron and the pump laser pulses. Figure 4 shows histograms of the rf amplitude and phase acquired over 2 hours. The rms relative jitter in the rf amplitude is 0.025%, while the rms jitter in the rf phase is 0.035 deg. The corresponding rms time-of-arrival-jitter is estimated to be <50 fs.

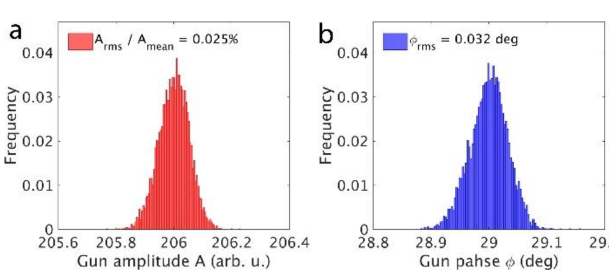

Figure 4: Histogram of rf amplitude (a) and phase (b) jitter acquired over 2 hours.

Electron Beam Pointing Stability

A good electron beam pointing stability is highly desirable to keep the spatial overlapping of electron beam, pump laser and gas target to make sure the diffraction data contains unambiguous information about the underlying ultrafast dynamics. To characterize the electron beam pointing stability, the exposure time of the electron detector was set to 4 ms to acquire single-shot electron images. The inset of Fig. 5 shows an example of the acquired single-shot electron profile. The centroids of the single-shot electron profiles are fitted with a Gaussian function and shown in Fig. 5. The rms pointing jitter in horizontal and vertical directions are 0.36 and 0.32 pixel, respectively. With a detector calibration factor of 35 um/pixel, the rms pointing jitter at the detector is ~10 µm. Tracking back to the interaction point at the gas chamber which is 3.1 meters upstream of the electron detector, the electron beam pointing jitter is estimated to be <10 µm.

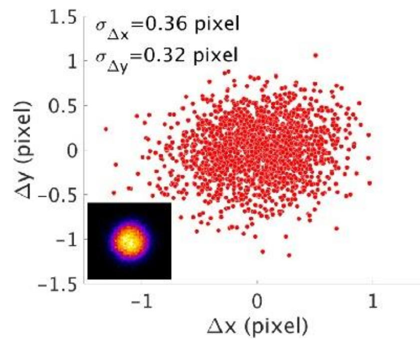

Figure 5: Electron beam pointing stability measured at the electron detector.

CONCLUSIONS

In summary, a MeV UGED system was commissioned at SLAC National Accelerator Laboratory with outstanding instrumental resolutions and machine stability. The MeV UGED system delivers electron beams of 3.7 MeV kinetic energy with 2 fC charge at 180 Hz repetition rate. A reciprocal-space resolution of 0.22 $Å^{-1}$ and a temporal resolution of 150 fs FWHM were achieved. The vacuum system is highly effective to provide 5-order-of-magnitude vacuum isolation between the gas chamber and the rf gun. The rms rf amplitude jitter is 0.025%, while the rms rf phase jitter is 0.032 deg. Electron beam pointing jitter is <10 µm.

To further improve the performance of the MeV UGED system, an rf compression cavity is proposed to compress the bunch length to 10-fs level, while the bunch charge is increased by more than a factor of 10 at the same time. A time-stamping technique [22] will be introduced to characterize the shot-to-shot arrival time jitter between the electron and the pump laser pulses, such that the diffraction data can be resorted to minimize temporal resolution degradation from such arrival time jitter. A direct electron detector [23] is under commission to enhanced the signal-to-noise performance of the gas diffraction pattern. Research and development efforts are dedicated for machine

ISBN: 978-3-95450-184-7 doi:10.18429/JACoW-IPAC2018-MOPML066

operation at 360 Hz or higher repetition rate for higher data acquisition efficiency.

ACKNOWLEDGEMENT

The authors are grateful to their SLAC colleagues for the strong management and technical support. This work was supported in part by the U.S. Department of Energy (DOE) Basic Energy Sciences Scientific User Facilities Division Accelerator & Detector R&D program under Contract No. DE-AC02-76SF00515, and the SLAC UED/UEM Initiative Program Development Fund.

REFERENCES

[1] P. Emma, *et al., Nat. Photonics,* 4, 641 (2010).
[2] T. Ishikawa, *et al., Nat. Photonics,* 6, 540 (2010).
[3] Y. Sakai, *et al.,* Phys. Rev. Accel. Beams 18, 1 (2015).
[4] X. J. Wang, *et al.,* in *Proceedings of 2003 Particle Accelerator Conference*, IEEE, Portland, OR, USA, 2003, pp. 420.
[5] X. J. Wang *et al., J. Korean Phys. Soc.* 48, 390 (2006).
[6] A. H. Zewail, *Annu. Rev. Phys. Chem.* 57, 65 (2006).
[7] A. H. Zewail, *Science* 328, 187 (2010).
[8] J. B. Hastings, *et al., Appl. Phys. Lett.* 89, 184109 (2006).
[9] R. K. Li, *et al., J. Appl. Phys.* 110, 074512 (2011).
[10] P. Musumeci, *et al., Appl. Phys. Lett.* 97, 063502 (2010).
[11] Y. Murooka, *et al., Appl. Phys. Lett.* 98, 251903 (2011).
[12] P. Zhu, *et al., New J. Phys.* 17, 063004 (2015).
[13] F. Fu, *et al., Rev. Sci. Instrum.* 85,083701 (2014).
[14] D. Filippetto, *et al.,* in *Proceedings of IPAC14*, Dresden, Germany, 2014, p. MOPRI053.
[15] S. Weathersby, *et al,. Rev. Sci. Instrum.* 86, 73702 (2015).
[16] X. Shen, *et al., Ultramicroscopy* 184, 172 (2018).
[17] A. H. Zewail*, J. Phys. Chem.* 100*,* 12701 (1996).
[18] J.C. Williamson, *et al., Nature* 386, 159 (1997).
[19] R. Srinivasan, *et al., Science* **307**, 558 (2005).
[20] J. Yang, *et al., Nat. Commun.*6, 8172 (2015).
[21] J. Yang, *et al., Faraday Discuss*. 7, 11232 (2016).
[22] M. Gao, *et al., Appl. Phys. Lett.* 103, 33503 (2013).
[23] T. Vecchione, *et al., Rev. Sci. Instrum.* 88, (2017).